Scientific paper

Origin of Drying Shrinkage of Hardened Cement Paste: Hydration Pressure

Ippei Maruyama[1]

Received 12 November 2009, accepted 6 May 2010

Abstract

The driving force of drying shrinkage of hardened cement paste has been attributed to $RT\ln(h)/v$ with external relative humidity h and water molar volume v in theories of capillary tension and disjoining pressure. However, these theories fail to explain the considerable hysteresis observed in length-change isotherms. In this study, the sorption isotherm and length-change isotherm of cement pastes were determined with different water-to-cement ratios and cement types, and internal pressure of shrinkage Π was calculated using the measured strain and elastic modulus of the skeleton. This internal pressure is a kind of disjoining pressure originated from hydration force and built up within adsorbed water films as a result of interactions between the hydrophilic solid surface and water molecules. Changes in internal surface energies of hardened cement pastes due to hydration, drying and temperature history result in a different statistical thickness of the adsorbed water layer under the same equilibrium relative humidity. The proposed model gives a rational explanation for the hysteresis in length-change isotherm.

1. Introduction

A volume change of concrete particularly associated with water evaporation is known as drying shrinkage. The drying shrinkage results in cracking of concrete under restraint conditions, and consequently spoils the appearance of concrete surface. It also increases the deflection of beams and slabs and induces the corrosion of rebars.

The mechanisms of volume change due to water content variation have been discussed extensively in terms of the experimental results and theories developed for other porous materials (i.e. Meeham 1927; Bangham and Fakhoury 1930; Hains and McIntosh 1947; Amberg and McIntosh 1952; Hiller 1964; Bentz *et al*. 1998). However, significant differences in sorption isotherm and length-change isotherm between hardened cement paste (hereafter referred to as hcp) and other porous materials are known to exist, as shown in **Fig. 1**, which compares porous glass (Amberg and McIntosh 1947) and hcp (Feldman and Sereda 1964). This figure shows that swelling of hcp during the adsorption process is smaller than shrinkage of hcp at the first desorption process, while porous glass exhibits quite the opposite tendency.

Despite extensive studies of the origin of shrinkage, no complete theory has been proposed so far, and combinations of several mechanisms have been commonly adopted to explain this phenomenon (Wittmann 2009).

The four most widely accepted shrinkage mechanisms include surface free energy (Feldman and Sereda 1964; Powers 1965; Powers 1968; Feldman 1968; Wittmann 1968; Feldman and Sereda 1970; Wittmann 1973), capillary tension (Powers 1965; Powers 1968), movement of interlayer water (Feldman 1968; Wittmann 1973; Feldman and Sereda 1968 and 1970) and disjoining pressure (Powers 1965; Powers 1968; Bazant 1972; Wittmann 1973; Ferraris and Wittmann 1987; Beltzung and Wittmann 2005). In recent work by Setzer (2007), several important points are made on the basis of unique experiments. First, hysteresis almost completely vanishes if length change is plotted as a function of mass change, and capillary pressure cannot be confirmed experimentally. Second, according to the measurement of density of hcp under different relative humidities, "there are strong indications that during the first desorption an irreversible change in surface interaction takes place and with it a change in the disjoining pressure." Finally, he concludes that the disjoining pressure is responsible to the shrinkage above approx. 30% RH and that hysteresis can be explained by the surface interaction between the water and gel during the first desorption.

Volume change of hcp may involve two factors to be addressed: one is the hysteresis phenomena. Generally, hysteresis is explained in terms of the ink-bottle concept, but additional shrinkage that is yielded by capillary tension (Schiller *et al*. 2008) can not be experimentally confirmed in hcp while it was observed in vycor glass. This implies that the ink-bottle effect is not dominant over the hysteresis of sorption isotherm. Even without ink-bottle effect, hysteresis can be explained by the changes of surface of hcp and resultant variation in the attraction force between water and the surface of hcp, as Setzer (2007) pointed out. The other factor is the driving force of volume change and associated constitutive low. Even if the bulk modulus, water content, and other parameters regarding volume change of hcp are given, existing models cannot predict the volume change be-

[1]Associate Professor, Graduate School of Environmental Studies, Nagoya University, Japan.
E-mail : ippei@dali.nuac.nagoya-u.ac.jp

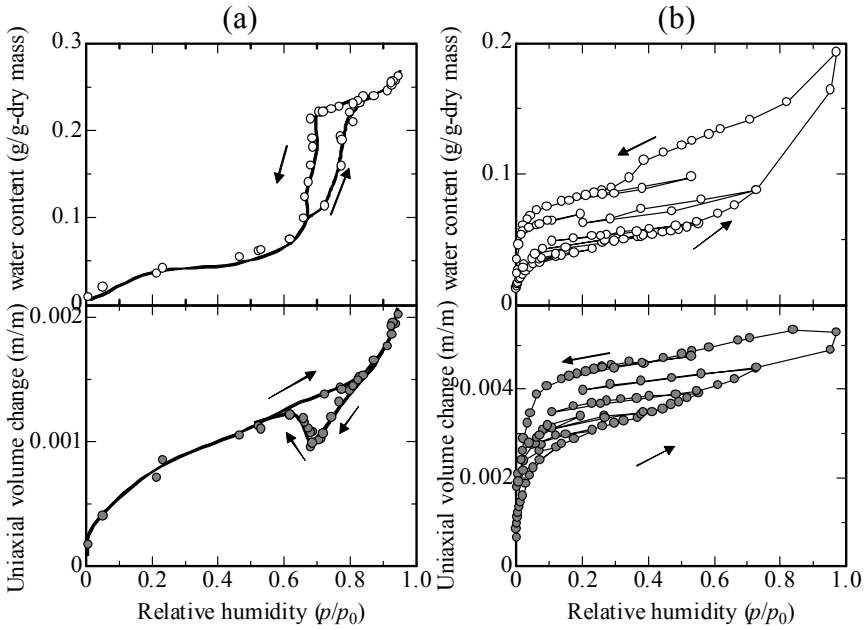

Fig. 1 Sorption isotherm and length-change isotherm of porous glass (a) and hardened cement paste (b). Data of porous glass is quoted from Amberg and McIntosh, and those of hardened cement from Feldman and Sereda.

havior particularly after hysteresis.

The present study mainly focuses on the general rule that can explain the volume change under given variations of water content and on the subsidiary hypothesis for hysteresis behavior using the experimental data. Because the most important experiment is sorption and length-change isotherms as Feldman (1968) pointed out, the length change and weight change isotherms of hcp, with three types of Portland cements and two different water-to-cement ratios, were determined. Next, these results were evaluated in terms of Derjaguin's disjoining pressure concept and relationship between statistical thickness of adsorbed water and the disjoining pressure was obtained experimentally.

2. Theory

Basic theories related to this experiment will be discussed first. The various experimental results and interpretations will then be presented to develop a new model. Finally, volume change of hcp will be discussed.

2.1 Disjoining pressure

Surface tension is caused by cohesion. Because the molecules on the surface of a liquid are not surrounded by like molecules on all sides, they are more attracted to their neighbors on the surface. In the classical theory by Gibbs, the basic thermodynamic form of the surface tension γ is defined by the change in free enthalpy G per area A

$$\gamma = \left(\frac{\partial G}{\partial A} \right)_{T,p,\mu} \tag{1}$$

where T = constant absolute temperature, p = pressure of the gaseous phase, and μ = chemical potential. But where hcp is concerned, the adsorption occurs in a small or regulated pore structure system and the adsorbed water in the small pore interacts with the skeleton of the hardened cement paste. This effect of the solid surface is not taken into account in Eq. (1).

Disjoining pressure Π, which takes into account the surface interaction, is defined by the change of surface enthalpy G' with the separation h of two interphases as

$$\Pi(h) = -\left(\frac{\partial G'}{\partial h} \right)_{p,T,\mu} \text{; with } G' = G / A \tag{2}$$

According to Derjaguin's definition, the disjoining pressure is the difference between the pressure under undisturbed bulk condition p_0 and the pressure at the interface p_1. And the pressure at the interface is defined by the forces acting perpendicular to the surface areas (Derjaguin and Churaev 1978).

$$\Pi(h) = p_1 - p_0 \tag{3}$$

Disjoining pressure is a general expression of interactions between surfaces at nano or sub-nano distances including all the interactive effects of solid, water, and dissolved ions. Components of disjoining pressure are categorized into three types of interaction forces, dis-

persive or molecular force, electrostatic force, and hydration force.

When two surfaces or particles get close within a few nanometers, continuum theories of van der Waals attraction and repulsive double-layer forces often fail to describe their interactions. This is either because one or both of these theories cannot work at a small distance or other non-DLVO forces come into play. Short-range oscillatory solvation forces arise whenever liquid molecules are induced to order into quasi-discrete layers between two surfaces or within any highly restricted space. And surface-solvent interactions can induce positional or orientational order in the adjacent liquid and give rise to a monotonic solvation force that usually decays exponentially with surface separation (Israelachvili 1991). This solvation force may be repulsive or attractive, and when the solvent is water, this type of structural forces is referred to as "hydration forces".

Repulsive hydration forces were originally found by Langmuir (1938) and can be seen in many materials, such as certain clays (van Olphen 1977), surfactant soap films (Cluine *et al*. 1967), uncharged liquid bilayers and biological membranes (McIntosh and Simon 1986). From existing experimental studies of silica, mica, certain clays and many hydrophilic colloidal particles, the hydration forces are believed to originate from strongly H-bonded surface groups such as hydrated ions or hydroxyl (-OH) groups.

The repulsive force acting between two silica surfaces in various aqueous NaCl solutions was experimentally confirmed by Grabbe and Horn (1993). It was found that the repulsive force decays exponentially with a decay length of approximately 1 nm. Their effective length was up to approximately 5 nm. Empirically, therefore, the hydration repulsion between two hydrophilic surfaces appears to follow a simple equation:

$$\Pi(e) = \Pi_0 \exp(-h/\lambda_0) \tag{4}$$

where λ_0 = decay length 0.3 to 1.0 nm, h = distance of surfaces, or double-thickness of adsorption, Π_0 = coefficient depending on the hydration of the surfaces, ranging from 80 to 23000 (MPa) as experimentally observed in mica, glass and quartz in various aqueous electrolyte solutions (Derjaguin and Churaev 1985).

Additionally, it should be noted that the Eq. (5) below, widely used in evaluating the disjoining pressure, is derived from two assumptions.

$$\Pi(e) = \frac{RT}{v}\ln(p/p_0) \tag{5}$$

where R = gas constant (J/mol/K), T = temperature in degrees Kelvin (K), v = molar volume of water (m^3/mol), p = vapor pressure at the existing state, and p_0 = the vapor pressure at the reference state of the system.

First, disjoining pressure is determined by the thickness of adsorption, and next the thickness of adsorption is determined by the ambient relative humidity and temperature. If the latter assumption is valid for the case of hcp, the sorption isotherm should be reversible. But in reality, the sorption isotherm shows hysteresis. Therefore, acknowledging that the mechanism of sorption hysteresis is not clear, the relationship between the thickness of the adsorbed layer and disjoining pressure could be the key issue in evaluating the volume change of hcp as a function of water content.

2.2 Equilibrium in hardened cement paste

The disjoining pressure between helium and glasses was measured by Sabisky and Anderson (1974) with a balance under gravitational potential. This means that the disjoining pressure can be evaluated by a mechanical balance.

The surface of hcp, which is mainly composed of C-S-H, is hydrophilic in nature. When water is adsorbed on the surface of a very narrow gap, repulsive force is produced. A schematic of this state is shown in **Fig. 2**

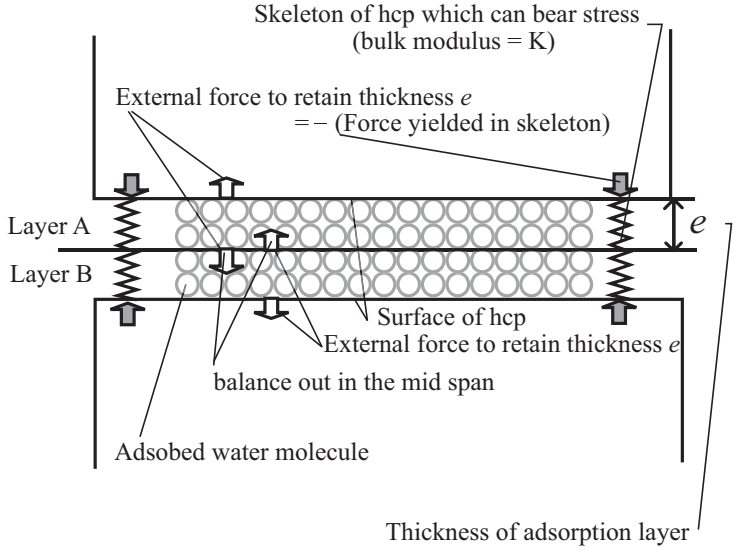

Fig. 2 Schematic of mechanical equilibrium in hardened cement paste.

where the pore structure is modeled with two parallel planes and the disjoining pressure, keeping the thickness of adsorbed layer constant, is balanced with the mechanical stress of the skeleton. It should be noted that the disjoining pressure is built by the adsorbed water in a homogeneous manner.

This balance in the system of hcp and water can be expressed as follows:

$$w\Delta\Pi = -K\frac{\Delta V}{V} \tag{6}$$

where w = volumetric water content (m^3/m^3) at the reference temperature, $\Delta\Pi$ = incremental change in disjoining pressure from the reference where the strain of hcp is zero (N/mm^2), K = bulk modulus of hcp (N/mm^2) (tentatively considered to be constant, this will be discussed later), and $\Delta V/V$ = volume change of hcp.

Generally, the value of disjoining pressure $\Pi(e)$ approaches zero as the thickness of adsorbed water e increases infinitely, and therefore even if hcp is in a saturated condition, the intrinsic disjoining pressure is not zero because the thickness of adsorbed water is a finite value.

2.3 Experimental approach

The saturated condition of hcp, referred to as state 1, is assumed to be the reference state for both disjoining pressure and strain. When the system is subjected to drying and reaches an equilibrium in an unsaturated condition, this condition is referred to as state 2. The difference in disjoining pressure $\Delta\Pi_{21}$ can be given by:

$$\Delta\Pi_{21} = -\left(\frac{K}{w_2}\cdot\frac{\Delta V_{21}}{V}\right) \tag{7}$$

where w_2 = volumetric water content at state 2, and $\Delta V_{21}/V_1$ = strain of volume change from state 1 to state 2. This equation is derived from Eq. (6). From this equation, the incremental disjoining pressure from the saturated condition is equal to the elastic force leading to the experimental determination of the disjoining pressure of the water in hcp.

Additionally, the bulk modulus of hcp K can be experimentally determined with axial loading test with longitudinal and vertical strain measurements:

$$K = \frac{E}{3(1-2\nu)} \tag{8}$$

where E = Young's modulus obtained from stress-strain relationship, and ν = Poisson's ratio obtained from strains of longitudinal and vertical directions.

Volumetric strain is evaluated with uniaxial strain from state 1 to state 2, $\Delta l_{21}/l_1$, as follows:

$$\frac{\Delta V_{21}}{V} = 3\cdot\frac{\Delta l_{21}}{l} \tag{9}$$

At the same time, the statistical thickness of adsorbed layer e can be experimentally obtained from specific surface area S (m^2/g-dry mass), water content by mass m_w (g-water/g-dry mass) and density of pore water ρ_w (g/m^3) as follows:

$$e = m_w/(\rho_w \cdot S) \tag{10}$$

Thus the relationship between incremental disjoining pressure $\Delta\Pi_{21}$ and statistical thickness of adsorbed layer e can be experimentally determined.

Possible questions of this experimental strategy may include, first the macroscopic approach shown as Eq. (6), second the statistical approximation of pore water, and finally the use of the first desorption. The macroscopic approach may be too simple to take into account all the local and microscopic interactions at various scales of pore size, which may lead to local relaxation and fine cracks during drying. However, the thermodynamic approach capable of describing the statistical nature of the hcp-water system is effective in discussing the mechanisms of volume change behavior of hcp. If the macroscopic volume change behavior of hcp is a result of interactions between hydration products and water at various pore scales, a statistically unique relationship can be expected between them and Eq. (6) can be applied as the first approximation. Assuming that statistically uniform cracks and local relaxations and resulting redistribution of stresses are present in the specimen, the fact that calculated disjoining pressure involves these effects and Eq. (6) has a limitation in separating these effects will be kept in mind in the subsequent discussion.

The statistical approximation of pore water may lead to disregard of the conventional distinction of adsorbed water and capillary-condensed water, because the statistical thickness of adsorbed water is simply calculated with moisture content by mass and specific surface area. However, all the water molecules in a saturated hcp are found to be within 2 nm from the solid surface, which is the working distance of disjoining pressure. Also, Setzer pointed out that the length change isotherms of hcp, if length changes are plotted against mass changes, are all the same regardless of the first desorption, first adsorption and second desorption. This implies that all the water molecules, even during desorption, are weakly structured under the influences of the surface forces.

Use of the first desorption may be unusual because the conventional studies presumed the dried state should be the reference state and started their experiments under highly dried conditions (Feldman 1968; Vlahinic *et al.* 2009), probably because the first desorption could result in some irreversible shrinkage strains, which would be inappropriate for the discussion of the shrinkage mechanisms. However, most of the existing concrete structures are at the first desorption and water molecules in hcp at this condition are more or less under some influences of disjoining pressure as stated above.

Hence the experimental results will be evaluated in terms of the relationship between statistical thickness of

adsorbed water and disjoining pressure.

3. Experiment

3.1 Specimen preparation

Ordinary Portland cement (notation N), moderate-heat Portland cement (M) and low-heat Portland cement (L) were mixed as a paste with a water-to-cement ratio of 0.55, 0.40 (notation 55 and 40 respectively). Those chemical compositions and properties are shown in **Table 1**. To minimize segregation, the paste was subjected to rotation for 6 hours until a creamy consistency was obtained, and was then cast in molds.

The specimens were placed in a thermostatic chamber at a temperature of 20 ± 1°C, demolded between 2 to 5 days and cured under saturated conditions until the test was commenced at 91 days of age.

3.2 Length-change and sorption isotherm

The specimens for length-change isotherm and sorption isotherm measurement were 3 × 13 × 300 mm in dimensions, which was referred to dimensions used in past experiments (Kondo 1958, Feldman 1964; Roper 1966; Mills 1966; Hansen 1987; Nagamatsu *et al*. 1992). It was reported that 10 mm thick hcp specimens made with ordinary Portland cement with a water-to-cement ratio of 0.40 at 28 days, reached an equilibrium within 28 days under controlled relative humidity (Kondo 1968), and that 4 mm thick hcp specimens required 14 days (Kondo 1968) to 20 days (Nagamatsu *et al*. 1992). Accordingly, the specimens in this experiment were stored in a controlled humidity chamber for 56 days. Because it was very difficult to control the relative humidity for the first 28 days after commencement of drying, the specimens had to be kept under constant controlled humidity for another 28 days.

The relative humidity in the chamber was controlled with a sodium hydrate solution. The targeted relative humidities were 98, 95, 90, 80, 70, 60, 50, 40, 30 and 20% at 20 ± 1°C. Concentrations of the solutions are tabulated in **Table 2** (Stokes and Robinson 1949) while these values are calibrated at the 25°C condition. The resulting relative humidities were monitored with a humidity sensor with a precision of 1.8% RH (Sensirion SHT75), and were controlled within 2% RH during the last half of 56 days. Major reason of using sodium hydrate was to avoid carbonation of hcp. Specimens were first conditioned under targeted humidities (98, 90, 80, 70, 60, 50, 40, 30% RH) and subjected to drying at 20% RH and finally returned to the original humidities (90, 80, 70, 60, 50, 40, 30% RH).

Table 2 Concentration of NaOH in aqueous solution and corresponding relative humidity.

Relative humidity (%)	Concentration (%mass)
95	5.54
90	9.83
80	16.10
70	20.80
60	24.66
50	28.15
40	31.58
30	35.29
20	40.00

Note: these values are experimentally confirmed at 25 °C (Stokes and Robinson 1949)

Length change was measured with a contact displacement meter with accuracy of 0.001 ± 1 mm. The deformation was determined by the difference with the reference of 300 mm in length made of invar. The measuring system is illustrated in **Fig. 3**. Deformation was reproducible to ± 15 × 10^{-6} strain. After the first drying at 20% RH, several samples were selected and subjected to oven-drying at 105°C for 24 hours, and the length change and amount of evaporable water loss were determined. More than five specimens were prepared for earch of the targeted conditions.

For sorption isotherm measurement, all the specimens were first dried at 105°C in an oven for 24 hours and water content at the saturated condition was determined. The amount of water adsorption was calculated using this oven-dry mass and loss of mass of drying specimen. Then the desorption isotherms of the first drying and the subsequent adsorption isotherm were measured. Mass losses were measured at a reproducibility of 0.1 mg. The volumetric water content was derived from the mass change, assuming that the density of adsorbed water is the same as that of the bulk water, i.e. 0.997g/cm^3, while pore water density of 1.15g/cm^3 was reported by Powers & Brownyard (1947), and recently water densities of approx. 1 g/cm^3 above 33% RH at the first desorption and 1.15-1.25 g/cm^3 at subsequent adsorption and desorption were reported by Setzer & Liebrecht (2007).

Table 1 Chemical composition and properties of cement.

	Density (g/cm^3)	Blaine alue (cm^2/g)	ig.loss (%)	Chemical Composition (%mass)								
				SiO_2	Al_2O_3	Fe_2O_3	CaO	MgO	SO_3	Na_2O	K_2O	Cl^-
Ordinary Portland cement	3.16	3110	0.64	21.8	4.49	2.90	63.9	1.84	2.26	0.20	0.38	0.007
Moderate heat Portland cement	3.21	3240	0.51	23.5	3.67	4.17	63.5	1.05	2.40	0.28	0.60	0.008
Low heat Portland cement	3.22	3470	0.71	26.3	2.65	3.04	63.3	0.71	2.42	0.16	0.32	0.004

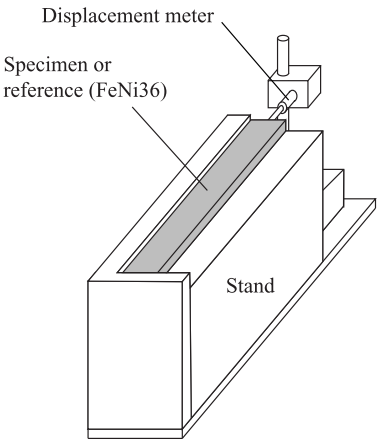

Fig. 3 Schematic of system for measuring length-change of specimen.

3.3 Surface area by water adsorption isotherm

Sorption isotherm of specimen at 91 days of age was determined with a pretreatment of oven drying at 105°C for 24 hours, and the surface area of hcp was calculated with the B.E.T. method. Water sorption measurements were performed with the volumetric method (Quantachrome Instruments Hydrosorb 1000).

3.4 Young's modulus, Poisson's ratio, and density of hcp

Specimens with a size of ϕ50 × 100 mm were prepared from the same batch of specimens subjected to length-change and sorption isotherm. Specimens were also cured under saturated conditions until the measurement at 91 days of age. Young's modulus was determined by a tangent of stress-strain relationship at the loading level of 1/3 of the maximum stress measured with a compresso meter.

The gauge length was 50 mm and the accuracy of the contact displacement meter was 0.001 mm. Poisson's ratio was measured with a wire-strain gauge attached mid height perpendicular to the loading direction. The resolution of the wire-strain gauge was 1 μ. Using Young's modulus and Poisson's ratio, the bulk modulus of the hcp at the saturated condition was calculated.

The bulk density of water-saturated hcp with a size of 5 mm cubic was measured by Archimedes' method at 20°C, and the true density of hcp was calculated from the bulk density and the water content.

4. Results and discussions

4.1 Experimental results and disjoining pressure curve

Figure 4 shows length-change strain with respect to the length in the saturated state as a function of relative humidity. Tabulated data are given in **Table A.1** in the Appendix. All the specimens show larger shrinkage strain in the adsorption process than in the virgin desorption process, similarly to the trend reported by Feldman *et al.* (1964). In almost all the cases, length change strains in the desorption process coincide with the strains in the adsorption process at a relative humidity lower than 40%. When the type of Portland cement is

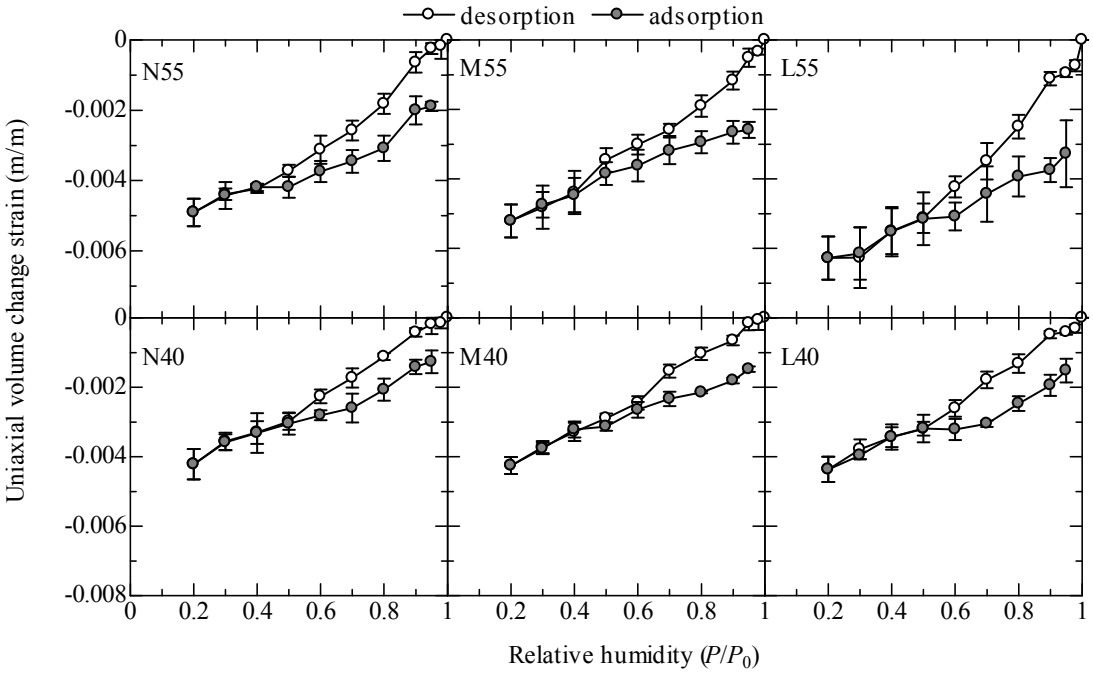

Fig. 4 Uniaxial length-change isotherm of hardened cement pastes.

Notation: N: Ordinary Portland cement, M: Moderate heat Portland cement, L: Low heat Portland cement, 55: Water to cement ratio of 0.55, 40: Water to cement ratio of 0.40

examined, Low heat Portland cement shows larger shrinkage in the desorption process, and this tendency is more conspicuous at a larger water-to-cement ratio.

Figure 5 shows the sorption isotherm of the specimen for the length-change isotherm. Tabulated data are given in **Table A.2** in the Appendix. The evaporable water is determined as the difference in mass of hcp between the saturated condition and oven-dry condition. Except for the case of L40, the amounts of adsorbed water in the desorption process coincide with those in the adsorption process at a relative humidity smaller than 40%, a trend similar to that of the length-change isotherm.

Figure 6 shows both the sorption isotherm of specimens dried in an oven at the age of 91 days and the virgin desorption isotherm of specimen for the length-change isotherm. The desorption data around 40% RH almost coincides, but certain discrepancies are observed in a range lower than 30% RH.

All the adsorption data lower than 30% RH showed good linearity on the B.E.T. plot and the specific surface area was obtained with a molecular area of 0.114 nm^2. The results are tabulated in **Table 3** with the other physical properties such as Young's modulus, Poisson's ratio, water content, and calculated bulk modulus and bulk density of hcps.

From these experimental data and Eqs. (7), (8), (9) and (10), the relationship between the difference in disjoining pressure $\Delta\Pi_{21}$ where state 1 is the saturated condition and state 2 is the arbitrary dried condition, and the statistical thickness of adsorbed layer e, can be derived. The results are shown in **Fig. 7** where the desorption and adsorption data can be arranged in the same curve. In former reaserch, it was reported that the relationship between $\Delta L/L$ (strain of length change) and $\Delta W/W$ (water content by mass) in the desorption process including several re-adsorption cycles can be represented in a single curve (Feldman 1968, Setzer 2007).

The regression curves of $\Pi_{21} = a \cdot \exp(-2e/b) - c$ applied to the experimental data are shown in **Fig. 7** as well. Even in the saturated condition, some disjoining pressure is assumed to be acting in hcp and this effect is represented as the term c. But for comparison or understanding the nature of those disjoining curves, the intrinsic curve is important. Therefore, intrinsic curves are obtained by eliminating the term c so that the disjoining curve approaches to zero when the statistical thickness of adsorbed layer increases infinitely.

The results of comparison are shown in **Fig. 8**. According to this figure, the following equation of disjoining pressure as a function of statistical thickness of adsorbed layer is derived:

$$\Pi(e) = 4500 \cdot \exp(-2e/0.95) \tag{11}$$

This empirical equation is similar to Eq. (4), and the experimental values λ_0 and Π_0 agree well with those of mica, glass and quartz reported by Derjaguin and Churaev (1985). Therefore, the cause of shrinkage of hcp might be attributed to the hydration force originated from the potential between adsorbed water and the surface of hydration products such as C-S-H. Because this type of disjoining pressure is not the same as those proposed in past studies, this pressure, supposed to dominate the drying shrinkage of cement paste, is named "hydration

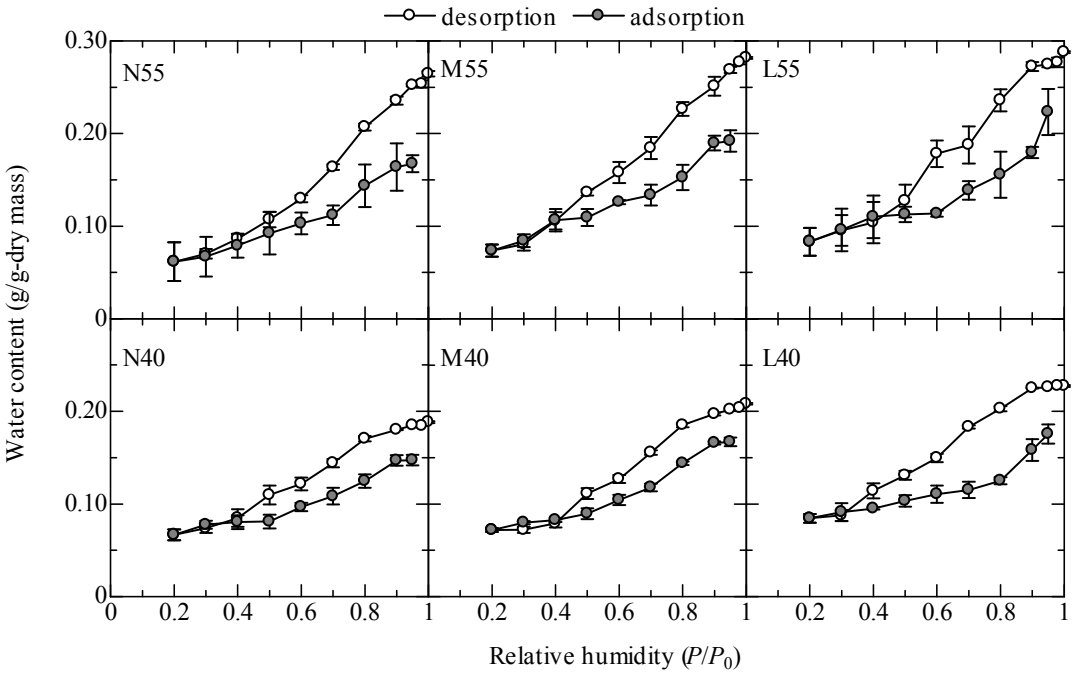

Fig. 5 Sorption isotherm of hardened cement pastes for length change isotherm.

Notation: N: Ordinary Portland cement, M: Moderate heat Portland cement, L: Low heat Portland cement, 55: Water to cement ratio of 0.55, 40: Water to cement ratio of 0.40

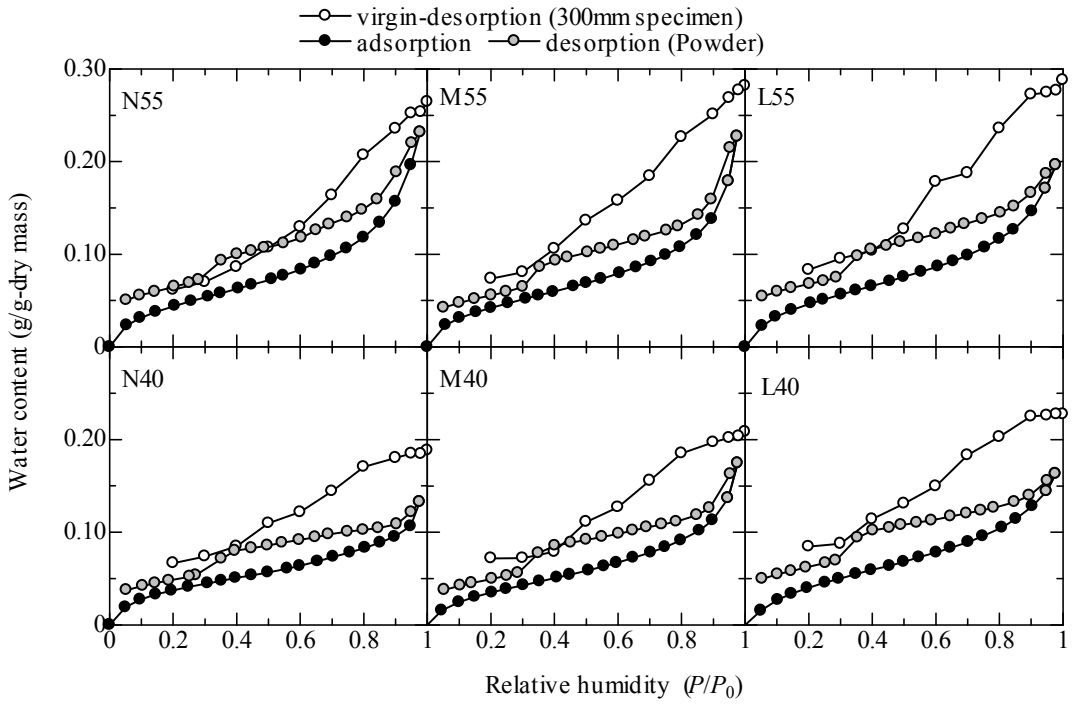

Fig. 6 Sorption isotherm of hardened cement pastes at the age of 91 days.

Notation: N: Ordinary Portland cement, M: Moderate heat Portland cement, L: Low heat Portland cement, 55: Water to cement ratio of 0.55, 40: Water to cement ratio of 0.40

Table 3 Physical properties of hardened cement pastes.

	Specific surface area (m^2/g)*1	Young's modulus (GPa)	Poisson's ratio	Bulk modulus (GPa)	Density (g/cm^3)	Water mass content at saturated condition (g/g)*2	Water volumetric content at saturated condition (cm^3/cm^3)*3
N55	160	15.1	0.261	10.5	2.56	0.264	0.404
N40	132	21.7	0.238	13.8	2.67	0.188	0.334
M55	152	14.9	0.275	11.0	2.67	0.281	0.429
M40	130	22.0	0.205	12.4	2.70	0.208	0.360
L55	173	13.3	0.260	9.27	2.66	0.288	0.434
L40	162	21.1	0.224	12.8	2.73	0.228	0.384

Note: *1, *2, *3: Reference is hcp dried at 105°C for 24 hours.

pressure".

The experimental data of Feldman (1968) as shown in **Fig. 1** is re-evaluated here to validate the proposed theory. Without the data of bulk modulus or Young's modulus of the hcp, it is possible to evaluate the relationship between the statistical thickness of the adsorbed layer and the strain over water content by mass ($(\Delta L/L)/w$), which should be linearly correlated to the hydration pressure. Using the tabulated adsorption data, the specific surface area of 125 m^2/g was obtained. **Figure 9** shows that the data of the adsorption and desorption processes can be arranged on the same curve except for one point, and their hydration pressure decay exponentially, while the decay lengths cannot be discussed because the statistical thickness of water depends on the method of surface area measurement and sample pre-treatment.

As shown in **Fig. 9**, the proposed theory of deformation of hcp at a relative humidity range from 20% to nearly 100% can be explained in terms of the hydration pressure originated from the hydration force.

Using Eq. (11) and the constitutive Eq. (6), the correlation between driving force of volume change, sorption behavior, and specific surface area is evaluated and shown in **Fig. 10**. Hcp with a large surface area shows higher sensitivity to the variation of statistical thickness of the adsorbed layer. It can be concluded that the volume change of hcp due to variation of water content is determined by 1) evaporability of water in hcp, 2) specific surface area, 3) hydrophilicity of surface of hydration products and 4) bulk modulus of hcp.

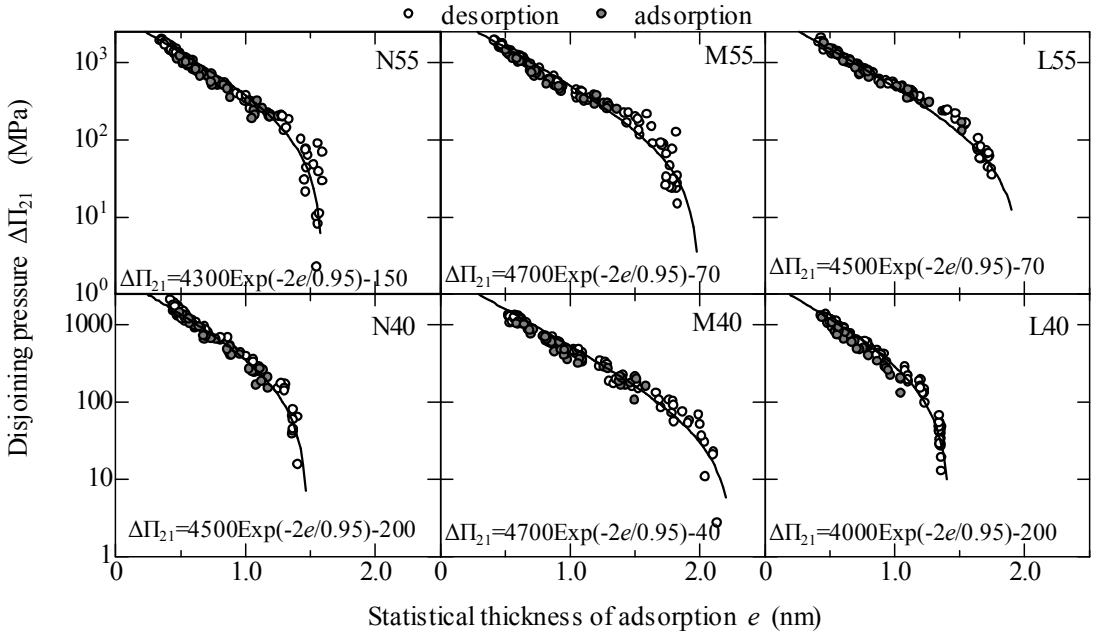

Fig. 7 Relationship between disjoining pressure and statistical thickness of adsorbed layer.

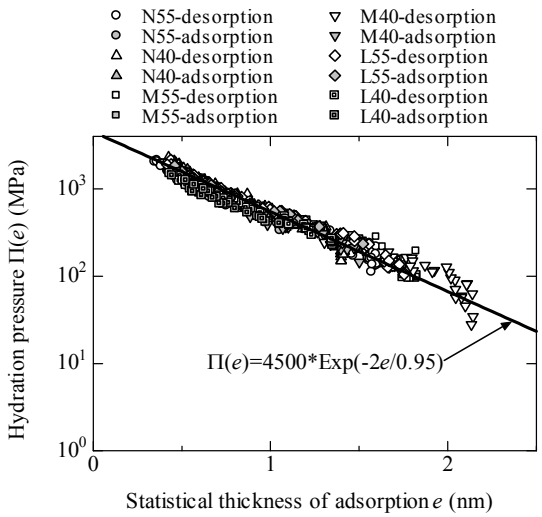

Fig. 8 Hydration pressure as a function of statistical thickness of adsorbed layer in hcp.

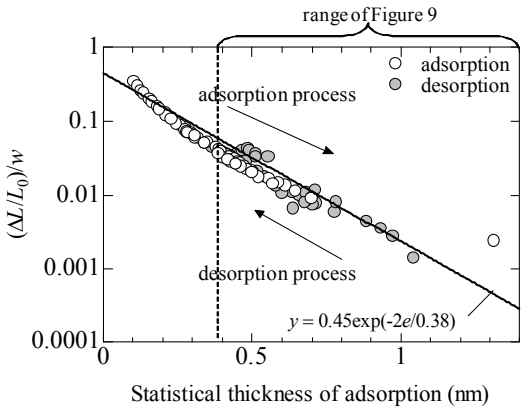

Fig. 9 Re-evaluation of Feldman's data by hydration pressure concept.

(Note: Starting point of this experiment was drying under 80℃ with degassing. Strain at 96.98% RH was assumed to be origin of deformation.)

Factors 1) and 3) above are probably interdependent, but the reason for sorption hysteresis and what determines the water content in hcp are not clear at this time, and therefore these two properties are treated independently.

4.2 Evaluation of the postulates

(a) Bulk modulus

In Eq. (7), the bulk modulus is assumed to be constant under variation of water content and ambient relative humidity. There is little experimental data of Young's modulus under different drying condition (Sereda *et al*. 1966; Wittmann 1973; Zech and Setzer 1988). Young's modulus measured under different relative humidities was normalized with that of the saturated or quasi-saturated condition and is shown in **Fig. 11**. Young's modulus decreases to 0.80 times that of the saturated condition. This can be attributed to the effect of creep, decomposition of hydration products, and micro-cracking. However, according to the experiment of Sereda *et al*., specimens were first dried under 0% RH condition, and a recovery in Young's modulus was confirmed as water was re-adsorbed, and thus the effect of micro-cracking seems to be minor. Additionally, Young's modulus also shows hysteresis according to the drying history, and therefore, the decomposition of hydration products may be a contributing factor to some extent.

Creep contribution is difficult to separate experimentally under loading test but may have some influence on this phenomenon. Regarding the proposed theory, it is obvious that the hydration pressure curves include the effect of variation in Young's modulus implicitly, and the obtained hydration pressure curve may be overestimated by up to approximately 25%. Further studies of the parameters are needed for a precise evaluation of the dependency of bulk modulus on relative humidity.

(b) Specific surface area

Determination of the surface area of hydrophilic colloidal materials always involves uncertainties because it leads to a separation between essentially fluid-like interfaces and the adsorbed water. However this has been resolved to some extent by directly measuring the electron density distribution across the aqueous phase (McIntosh and Simon, 1986).

Regarding C-S-H in hcp, it is also quite difficult to separate the physically adsorbed water and chemically bound water, for as an experiment, Klauss tried to determine the potential of water on C-S-H by the isobar test (Powers and Brownyard, 1947).

The specific surface area of hcp has been determined with different means and objectives, including water molecule, nitrogen molecule, X-ray, and neutron, and it was proven that the obtained surface area depends on the experimental method (Jennings 2000, Jennings *et al*. 2008). Because the volume change due to variation of water content is obviously caused by water, it is plausible that use of water molecule as a probe is rational for the determination of the specific surface area. However, the pretreatment drying condition of hcp specimens affects the result of the sorption isotherm. For example, in the case of specimens dried under d-dry condition for a very short time, hysteresis below 10% RH could not be seen (Powers and Brownyard 1947), while specimens degassed at 80°C showed large hysteresis above 0.2% RH (Feldman 1968), and specimens dried under 3% RH also showed hysteresis (Baroghel-Bouny 2007). At this time,

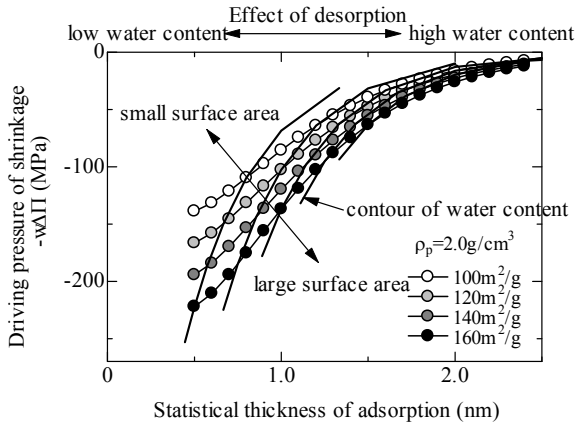

Fig. 10 Correlation of driving force of shrinkage, sorption, and specific surface area. In calculation, density of hcp is assumed to be 2.0 g/cm^3.

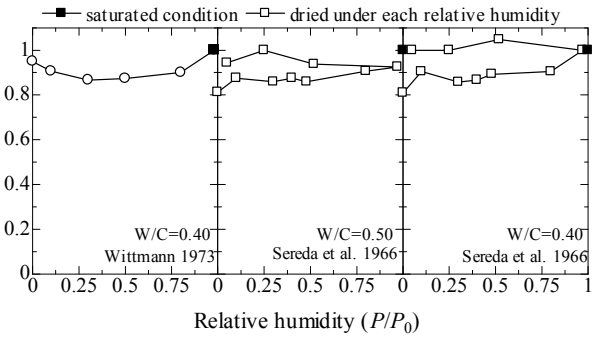

Fig. 11. Ratio of Young's modulus of hcp with equilibrium to different relative humidity to that of saturated or semi-saturated condition. Data are after Wittmann (1973) and Sereda *et al*. (1966).

determination of the surface area by the water adsorption method still involves difficulties of interpretation, and Eq. (11) is limited to the presented evaluation method of surface area.

4.3 Sorption, desorption and hysteresis

The drying process and surface area are focused on in the first place. Linearity can be found in B.E.T. plots of both the desorption and adsorption processes in the presented results. A typical example is shown in **Fig. 12**. A linear correlation between specific surface areas derived from the desorption isotherm and those from adsorption isotherm is shown in **Fig. 13**. It is likely that water adsorption sites increased after the specimen was subjected to a high relative humidity (97% RH was adopted for the sorption isotherm). Because porous materials do not generally show hysteresis under 33% RH, the hysteresis of hcp can be explained by the variation of surface area due to drying condition or drying history.

The specific surface area determined with SAXS (Small Angle X-ray Scattering) under different relative humidities showed similar trend, as shown in **Fig. 14** (Krop 1983, Hilsdorf 1984, Völkl *et al*. 1987). This figure indicates that even in a high relative humidity range, water adsorption sites are affected by the drying process. Therefore, the hysteresis of hcp is attributed to changes in water adsorption sites by the reaction of hydrates and the difference in activation energy between the drying and wetting processes.

Next, major causes changing the number of water adsorption sites are examined. In the case of silica-gel, it is experimentally confirmed with FT-IR (Fourier Transform Infrared Spectrophotometer) that the surface silanol is dehydrated to revive siloxane bonds under high temperatures (Kondo *et al*. 1984; Kondo 1986). The reaction at the surface of C-S-H could occur during drying and heating conditions as shown **Fig. 15**. Polymerization of silicate anions inside of C-S-H at a temperature as low as 50°C and associated irreversible volume changes are also inferred by Aono *et al*. (2007) using ^{29}Si NMR MAS and true density measurement. Thus, the main reaction re-

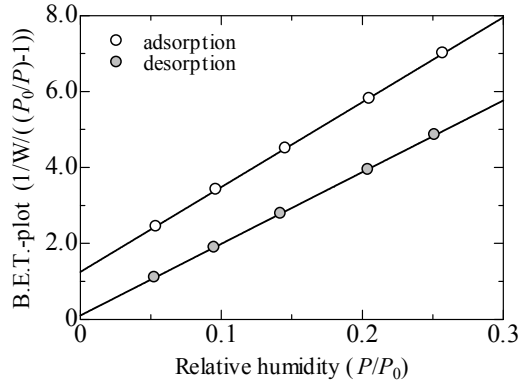

Fig. 12 B.E.T.-plot of adsorption and desorption isotherm of N55.

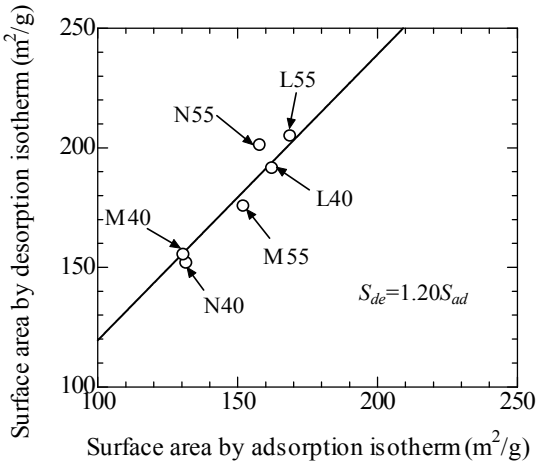

Fig. 13 Relationship between specific surface area calculated from desorption isotherm and that from adsorption isotherm.

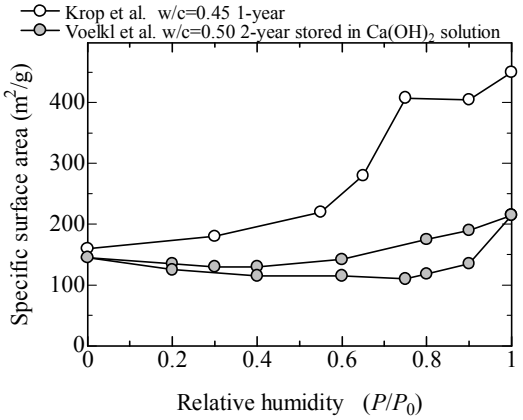

Fig. 14 Specific surface area by SAXS as a function of relative humidity. (after Krop *et al*. (1983) and Völkl *et al*. (1987)).

sponsible for the decrease in adsorption sites can be attributable to a chemical reaction between ≡SiOH and ≡Si-O-Si≡. The slight increase in adsorption sites below 40% RH in desorption process might be explained by the precipitation of SiO_2-ion under supersaturated conditions, which is supposed to be $H_6Si_4O_7^{2-}$ or $H_2SiO_4^{2-}$ in the high pH region (Dove 1995). On the contrary, in the adsorption process, the dissolution process of SiO_2-ion decreases the adsorption sites, while at a higher relative humidity range, inverse reactions of ≡Si-O-Si≡ to ≡SiOH should occur. A schematic of this phenomenon is shown in **Fig. 16**.

Compiling the above discussions, the hysteresis mechanism, which includes the irreversible strain mechanism of the first desorption, can be attributable to 1) difference in activation energy of reactions from ≡Si-O-Si≡ to ≡SiOH and reaction of SiOH to ≡Si-O-Si≡ (Renders *et al*., 1995), 2) process of precipitation and dissolution of SiO_2, although this is just a hypothesis that needs to be proved.

This study presents a novel approach to the volume changes of hcp and, on the basis of the disjoining pressure, shows that, starting from the saturated condition, the amount of water either adsorbed or reacted with C-S-H surfaces is the sole factor determining the volume change regardless of the first desorption or subsequent adsorption processes.

Unlike the widely accepted disjoining pressure concept, the proposed disjoining pressure comprises a hydration component that can take into account the effects of humidity changes on the solid surface that interacts with adsorbed water molecules and ions. This study is also characterized by the departure from the external humidity that was believed to solely control the statistical thickness of the adsorbed layer. A relationship between the length change of hcp and the statistical thickness of the adsorbed water, which represents the amount of water consumed either by adsorption on or reaction with the solid surface, was established.

5. Conclusions

The length-change isotherm and sorption isotherm of hcp with two water-to-cement ratios and three types of Portland cement were conducted to study the mechanism of volume change of hardened cement paste (hcp) due to variance of water content. The experimental results were evaluated separating the disjoining pressure concept from the external relative humidity and hysteresis issues, and the following equation was derived:

$$w\triangle\Pi + K\frac{\triangle V}{V} = 0,$$

where w = volumetric water content (m^3/m^3) at the reference temperature, $\Delta\Pi$ = incremental disjoining pressure from the reference (N/mm^2), K = bulk modulus of hcp (N/mm^2), and $\Delta V/V$ = volume change strain of hcp.

Based on this equation and the experimental results, disjoining pressure $\Pi(e)$ (= hydration pressure) as a function of statistical thickness e was obtained,

$$\Pi(e) = 4500\cdot\exp\left(-2e/0.95\right)$$

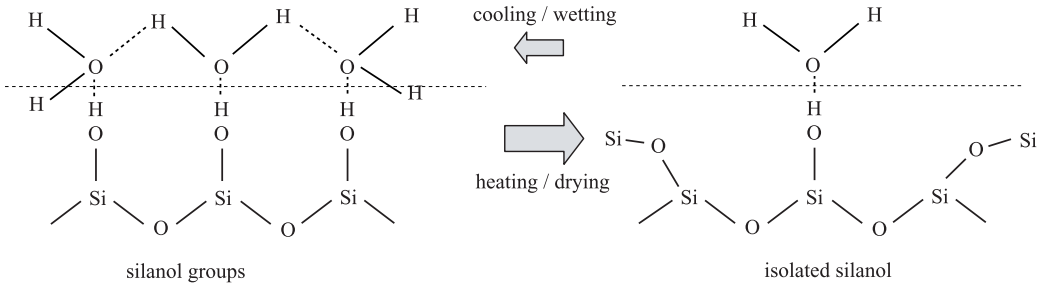

Fig. 15 Schematic diagram for water adsorption and silanol under different condition.

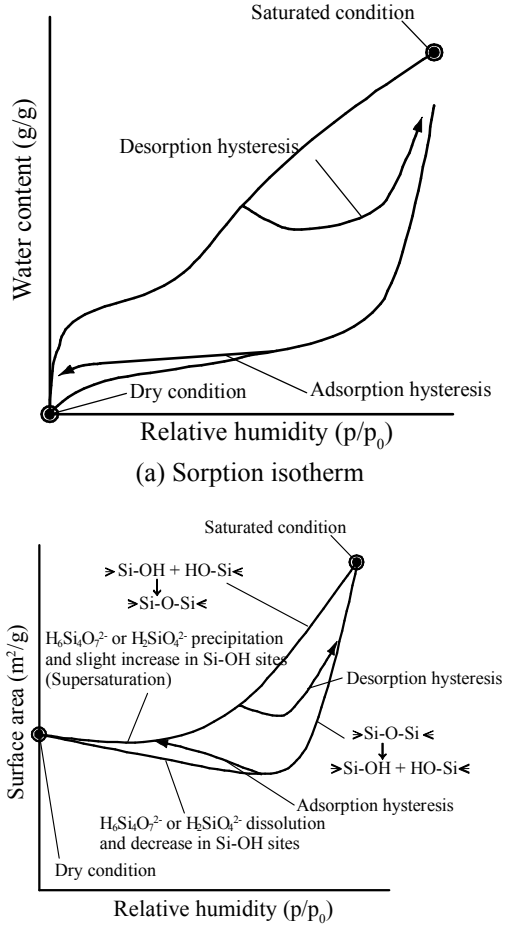

Fig. 16 Schematic of proposed hysteresis mechanisms. (Hysteresis envelope of surface area after Völkl *et al*. (1987)).

where the e = statistical thickness of adsorbed layer (nm), $\Pi(e)$ = hydration pressure (MPa).

The obtained disjoining pressure decays exponentially, showing a similar tendency to that of the "hydration forces" observed in many other hydrophilic substances, and is different from those proposed in past studies, and hence is named 'hydration pressure'.

The hydration pressure concept can be applied to the statistical thickness of the adsorbed water layer from 0.4 nm to 2.0 nm in hcp, while the calculation of statistical thickness of adsorbed water layer depends on the measurement of the surface area, which is affected particularly by the measuring method and pre-treatment drying of hcp. Therefore, the applicability of the obtained hydration pressure curve is limited.

The relationship between the hydration pressure and adsorbed water thickness obtained through the present experiments primarily shows how the solid surface interacting with adsorbed water and the ions adsorbed on the solid surface affect the statistical thickness of the adsorbed water layer. This study is characterized by the departure from the external humidity that was believed to simply control the statistical thickness of the adsorbed layer.

Acknowledgements

This research was mainly supported by the Japan Society for the Promotion of Science as part of project number 21686052, lead by Dr. I. Maruyama. The author expresses his sincere gratitude to Prof. D. Lange (University of Illinois) for information regarding relative humidity sensors, Dr. S. Tada (Texte, Inc.) for discussing the numerous aspects of existing phenomena in hardened cement paste such as the reactions of silanol groups, and Messrs. N. Kishi, A. Teramoto, and G. Igarashi (Nagoya Univ.) for performing numerous experiments and discussions.

References

Aono, Y., Matsushita, F., Shibata, S. and Hama, Y. (2007). "Nano-structural changes of C-S-H in hardened cement paste during drying at 50°C." *Journal of Advanced Concrete Technology*, 5(3), 313-323.

Amberg, C. H. and McIntosh, R. A. (1952). "A study of adsorption hysteresis by means of length changes of a rod of porous glass." *Canadian Journal of Chemistry*, 30, 1012-1031.

Bangham, D. H. and Fakhoury, N. (1930). "The swelling of charcoal. Part I. Preliminary experiments with water vapour, carbon dioxide, ammonia, and sulphur dioxide." *Proceedings of Royal Society of London, Series. A*, 130(812) , 81-89.

Baroghel-Bouny, V. (2007). "Water vapour sorption experiments on hardened cementitious materials Part I: Essential tool for analysis of hygral behaviour and its relation to pore structures." *Cement and Concrete Research*, 37, 414-437.

Bazant, Z. P. (1972). "Thermodynamics of hindered adsorption and its implications for hardened cement paste and concrete." *Cement and Concrete Research*, 2(1), 1-16.

Bentz, D. P., Garboczi, E. J. and Quenard, D. (1998). "Modeling drying shrinkage in reconstructed porous materials: Application to porous Vycor glass." *Modelling and Simulation in Material Science and Engineering*, 6, 211-236.

Beltzung, F. and Wittmann, F. H. (2005). "Role of disjoining pressure in cement based materials." *Cement and Concrete Research*, 35(12), 2364-2370.

Cluine, J. S., Goodman, J. F. and Symons, P. C. (1967). "Solvation forces in soap films." *Nature*, 216, 1203-1204.

Derjaguin, B. V. and Churaev, N. V. (1985). "Properties of water layers adjacent to interfaces." In: Croxton, C. A. Ed*., Fluid Interfacial Phenomena*, Chichester: John Wiley & Sons Ltd. 663-738.

Dove, P. M. (1995). "Kinetic and thermodynamic controls on silica reactivity in weathering environments." *Reviews in Mineralogy and Geochemistry*, 31 235-290.

Feldman, R. F. and Sereda, P. J. (1964). "Sorption of water on compacts of bottle-hydrated cement. I. The sorption and length-change isotherms." *Journal of applied Chemistry*, 14, 87-104.

Feldman, R. F. and Sereda, P. J. (1968). "A model for hydrated portland cement paste as deduced from sorption-length change and mechanical properties." *Materials and Structures*, 1(6), 509-520.

Feldman, R. F. (1968). "Sorption and length change scanning isotherms of methanol and water on hydrated Portland cement." *Proceedings of 5th International Symposium on Chemistry of Cement*, Tokyo, Part III, 53-66.

Feldman, R. F. and Sereda, P. J. (1970). "A new model for hydrated Portland cement and its practical implications." *Engineering Journal*, 53(8/9), 53-59.

Ferraris, C. F. and Wittmann, F. H. (1987). "Shrinkage mechanisms of hardened cement paste." *Cement and Concrete Research*, 17(3) 453-464.

Grabbe, A. and Horn, G. R. (1993). "Double-layer and hydration forces measured between silica sheets subjected to various surface treatments." *Journal of Colloid Interface Science*, 157, 375-383.

Hansen, W. (1987). "Drying shrinkage mechanisms in Portland cement paste." *Journal of American Ceramic Society*, 70(5), 323-328.

Haines R. S. and McIntosh, R. A. (1947). "Length change of activated carbon rods caused by adsorption of vapors." *Journal of Chemical Physics*, 15(1), 28-38.

Hiller, K. H. (1964). "Strength reduction and length changes in porous glass caused by water vapor adsorption." *Journal of Applied Physics*, 35. 1622-1628.

Hilsdorf, H. K., Krop, J. and Gunter, M. (1984). "Carbonation, pore structure and durability." In: *RILEM Seminar* Durability *of Concrete Under Normal Outdoor Exposure*, Hannover, 182-196.

Israelachvili, J. N. (1991). "*Intermolecular & Surface Forces*." 2nd ed., London: Academic Press.

Jennings, H. M. (2000). "A model for the microstructure of calcium silicate hydrate in cement paste." *Cement and Concrete Research*, 30, 101-116.

Jennings, H., Bullard, J. B., Thomas, J. J., Andrade, J. E., Chen, J. J. and Scherer, G. W. (2008). "Characterization and modeling of pores and surfaces in cement paste: Correlations to processing and properties." *Journal of Advanced Concrete Technology*, 6(1), 5-29.

Kondo, M. (1958). "Relationship between state of water in hardened cement paste and drying shrinkage by water evaporation." *Proceedings of Japan Cement Engineering Association*, 12, 136-149. (in Japanese)

Kondo, S., Yamaguchi, H., Kajiyama, Y. and Ishikawa, T. (1984). "Physical and chemical properties of inactive surface hydrogen-bonded hydroxyl groups," *Journal of Chemical Society, Faraday Transaction 1*, 80, 2033–2038.

Kondo, S. (1986). "Formation of colloidal silica and its properties of surface and pores." *Hyomen*, 24(4), 177-188. (In Japanese)

Krop, J., Grafenecker, T. and Hilsdorf, H. K. (1983). "Characterization of microstructure of hydrated cement paste by small angle X-ray scattering." In: Rossi-Doria, P. Ed., *Principles and applications of pore structural characterization*, Milan: RILEM/CNR, 339-363.

Langmuir, I. (1938). "The role of attractive and repulsive forces in the formation of tactoids, thixotropic gels, protein crystals and coacervates." *Journal of Chemical Physics*, 6, 873-896.

McIntosh, T. J. and Simon, S. A. (1986). "Hydration force and bilayer deformation: A Reevaluation." *Biochemistry*, 25(14), 4058-4066.

Meehan, F. T. (1927). "The expansion of charcoal on sorption of carbon dioxide." *Proceedings of Royal Society of London Series A*, 115(770), 199-207.

Mills, R. M. (1966). "Effects of sorbed water on dimensions, compressive strength and swelling pressure of hardened cement paste." *Proceedings of Symposium on Structure of Portland Cement Paste and Concrete*, Highway Research Board, Washington D. C., 84-109.

Nagamatsu, S., Sato, Y. and Ohtsune Y. (1992). "Relationship between degree of drying and drying shrinkage strain of hardened cement paste." *Journal of Structural and Construction Engineering*, AIJ, 439, 13-21. (in Japanese)

van Olphen, H. (1977). "*An introduction to clay colloid chemistry*." 2nd ed., New York: Wiley, chapter 10.

Renders, P. J. N., Gammons, C. and Barnes, H. L. (1995). "Precipitation and dissolution rate constants for cristobalite at 150 to 300℃." *Geochim. Cosmochim. Acta*, 59, 77-85.

Powers, T. C. and Brownyard, T. L. (1947). "Studies of the physical properties of hardened cement paste." Bulletin 22, *Research Laboratories of Portland Cement Association*.

Powers, T. C. (1965). "The mechanisms of shrinkage and reversible creep of hardened cement paste." *Proceedings of International Symposium of Structure of Concrete and its Behaviour under Load*, London, 319-344.

Powers, T. C. (1968). "The thermodynamics of volume change and creep." *Materials and Structures*, 1(6), 487-507.

Roper, H. (1966). "Dimensional change and water sorption studies of cement paste." *Proceedings of Symposium on Structure of Portland Cement Paste and Concrete*, Highway Research Board, Washington D. C., 74-83.

Sabisky, E. S. and Anderson, C. H. (1973). "Onset for superfluid flow in He^4 films on a variety of substrates." *Physical Review Letters*, 30(2), 1122-1125.

Sereda, P. J., Feldman, R. F. and Swenson, E. G. (1966). "Effect of sorbed water on some mechanical properties of hydrated Portland cement pastes and compacts." In. Proceedings *of Symposium on Structure of Portland Cement Paste and Concrete*, Highway Research Board, Washington D. C., 58-73.

Setzer, M. J. (2007). "The solid-liquid gel-system of hardened cement paste." In: Setzer M. J. ed., *Proceedings of Essen Workshop on* Transport *in Concrete: Nano- to Macrostructure*, Freiburg, Aedificatio Publisher, 3-23.

Setzer, M. J. and Liebrecht. A. (2007). "The CSH-gel - pore solution in hardened cement paste." In: Setzer M. J. ed., *Proceedings of Essen* Workshop *on Transport in Concrete: Nano- to Macrostructure*, Freiburg: Aedificatio Publisher, 207-215.

Schiller, P., Bier Th., Wahab, M. and Mögel, H. -J. (2008). "Mesoscopic model of volume changes due to moisture variations in porous materials." *Colloids and Surfaces A:* Physicochemical *and Engineering Aspects*, 327(1-3), 34-43.

Stokes, R. H. and Robinson, R. A. (1949). "Standard solutions for humidity control at 25°C." *Industrial and Engineering Chemistry*, 41(9), 2013.

Vlahinic, I., Jennings, H. M. and Thomas, J. J. (2009). "A constitutive model for drying of a partially saturated porous material." *Mechanics of Materials*, 41(3), 319-328.

Völkl, J. J., Beddoe, R. E. and Setzer, M. J. (1987). "The specific surface area of hardened cement paste by small-angle X-ray scattering-Effect of moisture content and chlorides." *Cement and Concrete Research*, 17, 81-88.

Wittmann, F. H. (1968). "Surface tension shrinkage and strength of hardened cement paste." *Materials and Structure*, 1(6), 547-552.

Wittmann, F. H. (1973). "Interaction of hardened cement paste and water." *Journal of American Ceramic Society*, 56(8), 409-415.

Wittmann, F. H. (2009). "Heresies on shrinkage and creep mechanisms." In: Tanabe *et al*. Ed., *Proceedings of Creep, Shrinkage and Durability Mechanics of Concrete and Concrete Structures*, London: Taylor and Francis Group, 3-10.

Zech, B. and Setzer, M. J. (1988). "The dynamic elastic modulus of hardened cement paste. Part 2. Ice formation, drying and pore size distribution." *Materials and Structure*, 22, 125-132.

Appendix: Experimental data

Table A.1 Sorption isotherms.

RH	N55 (g/g)	N40 (g/g)	M55 (g/g)	M40 (g/g)	L55 (g/g)	L40 (g/g)
1.00	0.2645	0.1884	0.2818	0.2083	0.2880	0.2275
0.98	0.2536	0.1843	0.2769	0.2036	0.2768	0.2274
0.95	0.2522	0.1849	0.2689	0.2019	0.2746	0.2260
0.90	0.2355	0.1802	0.2511	0.1972	0.2724	0.2251
0.80	0.2070	0.1705	0.2266	0.1851	0.2360	0.2030
0.70	0.1637	0.1442	0.1843	0.1557	0.1877	0.1833
0.60	0.1296	0.1217	0.1580	0.1270	0.1782	0.1497
0.50	0.1071	0.1098	0.1364	0.1112	0.1272	0.1309
0.40	0.0865	0.0848	0.1058	0.0790	0.1039	0.1142
0.30	0.0701	0.0738	0.0806	0.0721	0.0953	0.0877
0.20	0.0616	0.0666	0.0737	0.0719	0.0832	0.0846
0.30	0.0671	0.0776	0.0843	0.0799	0.0959	0.0913
0.40	0.0790	0.0804	0.1065	0.0828	0.1101	0.0952
0.50	0.0924	0.0811	0.1093	0.0896	0.1127	0.1033
0.60	0.1029	0.0968	0.1260	0.1044	0.1136	0.1106
0.70	0.1119	0.1083	0.1335	0.1178	0.1385	0.1152
0.80	0.1436	0.1247	0.1527	0.1440	0.1556	0.1253
0.90	0.1639	0.1470	0.1896	0.1659	0.1795	0.1584
0.95	0.1674	0.1473	0.1920	0.1670	0.2233	0.1756

Table A.2 Length-change isotherms.

RH	N55 (m/m)	N40 (m/m)	M55 (m/m)	M40 (m/m)	L55 (m/m)	L40 (m/m)
1.00	0.000000	0.000000	0.000000	0.000000	0.000000	0.000000
0.98	-0.000169	-0.000169	-0.000337	-0.000063	-0.000740	-0.000311
0.95	-0.000245	-0.000245	-0.000512	-0.000154	-0.000959	-0.000410
0.90	-0.000641	-0.000641	-0.001171	-0.000653	-0.001117	-0.000482
0.80	-0.001818	-0.001818	-0.001901	-0.001033	-0.002498	-0.001321
0.70	-0.002574	-0.002574	-0.002588	-0.001533	-0.003489	-0.001789
0.60	-0.003121	-0.003121	-0.003012	-0.002449	-0.004235	-0.002608
0.50	-0.003720	-0.003720	-0.003454	-0.002895	-0.005133	-0.003195
0.40	-0.004228	-0.004228	-0.004394	-0.003287	-0.005505	-0.003435
0.30	-0.004387	-0.004387	-0.004819	-0.003726	-0.006270	-0.003789
0.20	-0.004906	-0.004906	-0.005210	-0.004255	-0.006282	-0.004366
0.30	-0.004423	-0.004423	-0.004747	-0.003763	-0.006147	-0.003963
0.40	-0.004189	-0.004189	-0.004469	-0.003218	-0.005524	-0.003432
0.50	-0.004183	-0.004183	-0.003849	-0.003130	-0.005149	-0.003187
0.60	-0.003738	-0.003738	-0.003618	-0.002649	-0.005084	-0.003218
0.70	-0.003452	-0.003452	-0.003193	-0.002333	-0.004434	-0.003049
0.80	-0.003079	-0.003079	-0.002947	-0.002150	-0.003932	-0.002471
0.90	-0.002001	-0.002001	-0.002659	-0.001807	-0.003747	-0.001944
0.95	-0.001888	-0.001888	-0.002589	-0.001479	-0.003273	-0.001518
0.00*	-0.009149	-0.007093	-0.009317	-0.007858	-0.01190	-0.009425